Nuclear Instruments and Methods in Physics Research A 789 (2015) 134–142

Contents lists available at ScienceDirect

Nuclear Instruments and Methods in Physics Research A

journal homepage: www.elsevier.com/locate/nima

A scintillator based endcap K_L and muon detector for the Belle II experiment

T. Aushev [a,b,c], D.Z. Besson [a,d,*], K. Chilikin [a,b], R. Chistov [a,b], M. Danilov [a,b], P. Katrenko [a,b], R. Mizuk [a,b], G. Pakhlova [a,b], P. Pakhlov [a,b], V. Rusinov [a,b], E. Solovieva [a,b], E. Tarkovsky [a,b], I. Tikhomirov [a,b], T. Uglov [a,b,c]

[a] National Research Nuclear University MEPhI (Moscow Engineering Physics Institute), Kashirskoye shosse 31, Moscow 115409, Russia
[b] Institute for Theoretical and Experimental Physics, B. Cheremushkinskaya 25, Moscow 117218, Russia
[c] Moscow Institute of Physics and Technology, Institutskiy per. 9, Dolgoprudny, Moscow Region 141700, Russia
[d] University of Kansas, Department of Physics and Astronomy, 1082 Malott Hall, Lawrence, KS 66045, USA

ARTICLE INFO

Article history:
Received 26 October 2014
Received in revised form
10 February 2015
Accepted 22 March 2015
Available online 15 April 2015

Keywords:
Plastic scintillator detectors
Particle tracking detectors
SiPM
Muon detector

ABSTRACT

A new K_L^0 and muon detector based on scintillators will be used for the endcap regions in the Belle II experiment, currently under construction. The increased luminosity of the e^+e^- SuperKEKB collider entails challenging detector requirements. We demonstrate that relatively inexpensive polystyrene scintillator strips with wavelength shifting fibers ensure a sufficient light yield at the Silicon PhotoMultiplier (SiPM) photodetector, are robust and provide improved physics performance for the Belle II experiment compared to its predecessor, Belle.

1. Overview

Over the last decade, the B-factory experiments, Belle and BaBar, have shown that flavor physics has the powerful potential to search for various manifestations of New Physics. If the statistical errors of measurements in the flavor sector can be substantially improved, the energy scale of New Physics studies can be pushed beyond 1 TeV, providing strong impetus for construction of the next generation B-factory. The idea of an upgraded Belle experiment was first presented in a Letter of Intent in 2004 [1], followed by a Technical Design Report in 2010 [2]. In parallel, the KEKB accelerator group has defined the parameters of the SuperKEKB accelerator, an upgraded version of KEKB, with luminosity increased by almost two orders of magnitude, and an ultimate instantaneous luminosity goal of $8\times10^{35}\ \mathrm{cm}^{-2}\ \mathrm{s}^{-1}$. Currently the SuperKEKB Factory, and the associated Belle II subdetectors are under construction at the High Energy Accelerator Research Organization, KEK, in Tsukuba, Japan. This new installation is expected to begin operation at the end of 2015 with the goal of collecting an integrated luminosity of 50 ab^{-1} by 2020.

The K_L^0 and muon subsystems (KLM) in the Belle experiment were designed to detect K_L^0 mesons and muons as they traversed the segmented flux return of the Belle solenoid, using resistive plate chambers (RPC) [3,4]. The KLM system has a cylindrical (barrel) part and two planar endcap sections. The RPC KLM detector operated successfully over the entire lifetime of Belle (1999–2010). However, the endcap KLM gas detectors of the Belle II experiment would suffer considerably compromised performance in the higher luminosity SuperKEKB environment, given the higher backgrounds and the long RPC dead times. This requires development of a new detection technique, which should be robust, inexpensive and capable of coping with high backgrounds.

In this paper, we present a scintillator-based solution for the Belle II endcap KLM (EKLM) detector and demonstrate that it matches the scientific and environmental requirements. The prospects for this technology were first discussed in a previous paper [5], after which this technology was chosen as the baseline technology for Belle II. Considerable R&D studies have been performed in order to demonstrate the feasibility of the proposed approach, and the construction of the new EKLM detector is already underway. A similar approach was also proposed for the SuperB experiment in Italy [6], which has since, quite unfortunately, been terminated.

2. The Belle II EKLM system

The Belle II EKLM system will follow its Belle predecessor, consisting of alternating layers of active charged particle detectors

* Corresponding author.
E-mail address: zedlam@ku.edu (D.Z. Besson).

http://dx.doi.org/10.1016/j.nima.2015.03.060
0168-9002/

and 4.7 cm thick iron plates. The iron plates serve as the magnetic flux return for the solenoid and provide a total of 3.9 interaction lengths of material for a particle travelling normal to the detector planes. There are 14 detector and 15 iron layers in each of the forward and backward endcaps. Each detector layer is divided into 4 sectors, which can be separately installed. Since the Belle iron structure will be retained, we plan to simply swap in our new detector, subject to the constraint that it must mate with the existing sector frames which guide installation into the 4.0 cm wide iron gaps.

Scintillator counters with wave-length-shifting (WLS) fibers as a readout option for the EKLM were first proposed by our group in the Belle upgrade Letter of Intent [1]. Charged particle detection with such detectors, equipped with photomultiplier tube (PMT) readout, is a well-established technique [7,8]. However, in the case of the Belle II detector, the limited space and the strong magnetic field do not allow use of PMTs. As an alternative photodetector, we proposed multipixel silicon photodiodes operating in the Geiger mode, originally developed in Russia [9] in the 1990s, and currently produced by many companies under different names: Silicon PhotoMultiplier (SiPM), Avalanche Photo-Diodes (APD), Metal-Resistor-Semiconductor (MRS), Multi-Pixel Photon Counters (MPPC), Multi-Pixel Avalanche Photo-Diodes (MAPD), among others. In this paper, we will use the generic name SiPM to include all such detectors.

SiPMs allow for compact detectors and uncompromised operation in strong magnetic fields. The first large-scale (7620 channels) SiPM application was the CALICE experiment's hadron calorimeter [10,11], which demonstrated the feasibility to use SiPMs experimentally, as well as their advantages over traditional PMTs. The use of SiPMs in a real experiment with a huge number of readout channels (~65 k) began with the near detector of the T2K experiment [12], where many subsystems are based on SiPM readout of scintillator light. However, the background rates and the radiation environment in neutrino experiments are much more benign, and therefore more stringent testing is required to prove the applicability of this technique to the more exacting Belle II environment.

2.1. General layout

The base element of the new detector system is a scintillator strip of polystyrene doped with a scintillator die. It has a rectangular cross-section and a varying length of up to 2.8 m to match the geometry of an individual sector. The strip height is limited to 10 mm by the mechanical constraints of the gap between the iron yoke and the frame structure. The selected strip width of 40 mm is a compromise between the desire for a moderate number of channels and the required spatial resolution for muon and K_L^0 reconstruction. The granularity is similar to the average granularity of the Belle experiment's original RPCs. It is commensurate with the uncertainties due to muon multiple scattering and typical hadron shower transverse sizes; further increase of the granularity does not improve muon identification performance and K_L^0 angular resolution. The hit registration efficiency does not depend on the strip width as long as the rates remain below data acquisition (DAQ) and SiPM saturation levels.

A schematic of the assembled strip is shown in Fig. 1. Individual strips are covered with a diffuse reflective coating; each strip has a groove in the center to accommodate a WLS fiber. Scintillator light is collected by a WLS fiber and transported to the photodetector. Each WLS fiber is read out from one (near) side – the far end of the WLS fiber is mirrored to increase the total light yield from the strip. To increase the efficiency for light collection, the WLS fiber is glued to the scintillator with optical glue. The SiPM is then coupled to the fiber end, and fixed and aligned with the fiber using a plastic housing.

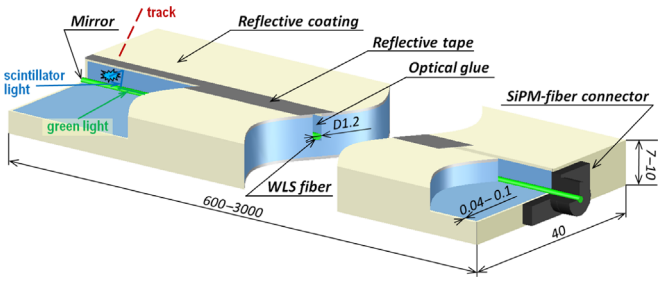

Fig. 1. Schematic view of the scintillator strip. Dimensions are in mm.

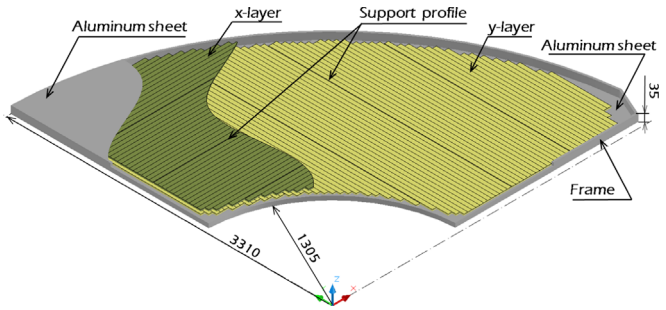

Fig. 2. Schematic view of one superlayer formed by scintillator strips. Sizes are given in mm.

One superlayer is formed from two fully overlapping orthogonal layers, each containing 75 scintillator strips. The independent operation of two planes in one superlayer should reduce the combinatorial background in comparison with the present RPC design, where every background hit produces signals in both readout planes. Scintillator strips are arranged in a sector, with a geometry matched to the existing gap in the iron yoke, as shown in Fig. 2. Fifteen strips are glued to a common thin (1.5 mm) polystyrene substrate from both sides and fixed in the support profile. In addition to providing rigidity and moderate passive neutron shielding, this substrate also serves to absorb protons scattered by background neutrons, and thereby prevents correlated hits in two layers appearing from a single background neutron. The sector frame is the same as that used for Belle's RPC mounting. The dead zone around the inner arc is estimated to be ~1% of the total sector area due to the inscription of the rectangular structure into the circular housing; this inner dead zone is approximately the same as that of the Belle RPC EKLM detector. Around the outer circumference, the dead zone is 4%, primarily owing to the presence of front-end electronics and cables. In practice, this dead area cannot be recovered, as the extremely short strips that might be installed there have very small coverage, and do not justify the additional number of readout channels they would entail.[1] In the middle part of the sector, unavoidable small dead zones (0.8%) are due to the presence of support structures. The total insensitive area between strips due to the reflective cover is only 0.3%. In total, the geometrical acceptance of the new system is slightly better than that of the Belle RPC EKLM.

In the new EKLM system the scintillator-based superlayers are installed in all 14 gaps in the magnet yoke in both the forward and backward endcaps. The entire system consists of 16,800 scintillator strips of varying lengths.

[1] We note that the acceptance loss at large radii is not critical for muon and K_L^0 reconstruction.

2.2. SiPMs, detailed description

A SiPM is a matrix of tiny photo-diodes (pixels) connected to a common bus and operating in the Geiger mode [9]. Photographs of SiPM surfaces, comparing samples from different vendors, are shown in Fig. 3. The number of pixels is ~100–1000, over a typical area of $1 \times 1\ \mathrm{mm}^2$. Connection to the common bus is generally achieved via a ~MΩ resistor. This resistor limits the Geiger discharge developed in a pixel by photo- or thermal electrons. In this mode, the SiPM response depends on the number of fired pixels and is proportional to the initial light, as long as the number of fired pixels is much smaller than the total number of pixels.

As compared with conventional vacuum photomultipliers, SiPMs have lower operating voltages, typically of the order a few tens of volts, which is higher than the breakdown threshold by several volts. The values of the overvoltage and the capacitance of a single pixel determine the photo-detector gain (typically of order 10^6). The values of quenching resistance and the capacitance of a single pixel determine the dead time of a pixel, which is typically ~10–100 ns. The photon detection efficiency (*PDE*) depends on the overvoltage and reaches 30–40% for modern devices. SiPMs with a smaller number of pixels usually have higher *PDE* values owing to the smaller non-sensitive area between pixels. The insensitivity of our SiPM samples to magnetic fields was checked in fields up to 4 T [16].

Among the disadvantages of SiPMs are the high levels of noise ($\sim 10^5$–10^6 Hz/mm^2 at a 0.5 photoelectrons (p.e.) threshold), an optical inter-pixel cross-talk producing a tail of large noise amplitudes, and high sensitivity of the SiPM response to ambient temperature, since the breakdown voltage depends on temperature (~60 mV/K for Hamamatsu, ~20 mV/K for CPTA).

A comparison of the measured SiPM characteristics from different vendors is shown in Fig. 4. The photon detection efficiency for green light from the Y11 WLS fiber, gain, cross-talk, and noise rate is shown as a function of overvoltage for detectors produced by MEPhI/PULSAR (Russia), CPTA (Russia) (CPTA 143), and Hamamatsu (Japan) (MPPC S10362-13-050). For these measurements, we used a calibrated light source which was being monitored with a standard PMT. The presented characteristics are extracted from fits to the randomly triggered (to collect noise) and externally triggered (synchronized with light source pulses) ADC spectra. The spectrum of the number of fired pixels for externally triggered data is fitted to a Poisson distribution convolved with a cross-talk correction. In this way, we extract both *PDE* from the Poisson mean, and the cross-talk value independently. To minimize statistical fluctuations, the data shown are averaged over 10–50 specimens from each vendor. While the breakdown voltage varies for individual specimens, the dependence on overvoltage ($\Delta V = V - V_{\text{break down}}$), in general, has a very small dispersion; $V_{\text{break down}}$ itself can be determined from extrapolation assuming a linear gain dependence on voltage.

MEPhI/PULSAR SiPMs were developed much earlier than other mass produced SiPMs, and their efficiency is correspondingly somewhat lower than the more advanced models. SiPMs produced by CPTA and Hamamatsu meet our minimum requirements, defined as high detection efficiency for Minimum Ionizing Particles (MIP) and low cross-talk. In spite of the higher observed single pixel noise for CPTA SiPMs, their smaller cross-talk value results in a relatively low noise rate, of the order of kHz, at a 7.5 p.e. threshold. It should be noted that the noise rate is not critical for our system, since at the chosen threshold, the main background arises from neutrons, rather than SiPM noise. Both CPTA and Hamamatsu were considered as the primary SiPM vendors for the T2K experiment, and both vendors have produced thousands of SiPMs that mate to our 1.2 mm diameter fiber. Our choice between these two (both acceptable) vendors was made based on a radiation hardness study as described in Section 3.2.

2.3. Scintillator strips

The largest light yield in the blue regime is achieved with organic scintillators, *e.g.* those produced by Bicron [17]. However, the production technique for such scintillators does not allow production of individual long strips, which can only be achieved by gluing together short strips, and is also very expensive to be practically considered for a detector having the large area of the Belle II EKLM system ($> 1000\ \mathrm{m}^2$). Therefore, we have focused on achieving sufficient light yield with much less expensive polystyrene scintillators.

Scintillator strips made of polystyrene, typically doped with PTP (p-terphenil) or PPO (2,5-diphenyloxazole) and POPOP (1,4-bis-2-(5-phenyloxazolyl)-benzene), can be produced by extrusion, in principle allowing manufacture of very long strips. Although different vendors use slightly different ingredients and production techniques, they generally achieve quite similar quality, and have similar prices. We tested the characteristics of scintillator strips from three vendors: Amkris-Plast (Kharkov, Ukraine) [18], which produced the strips in use for the Opera experiment [8], Fermilab (USA) [19], and also Uniplast (Vladimir, Russia) [20], which both produced the scintillator strips for the T2K experiment [12]. All strips had width 40 mm. The height of the Amkris-Plast and Fermilab strips was 10 mm, and the thickness of the co-extruded TiO_2 + polystyrene coating was ~100 microns. For the third vendor, we used existing Uniplast strips produced for the T2K experiment with 7 mm thickness. The reflection coating is achieved in this case by chemical etching of the surface and is thinner (40–50μ).

In all tested strips, Kuraray WLS Y-11(200)MSJ multi-cladding 1.2 mm diameter fibers [21] were glued using SL-1 glue produced at SUREL (St. Petersburg, Russia) [22]. The Kuraray fiber provides more light output than other fibers and also has a favorably long attenuation length. This fiber has been used in many detectors

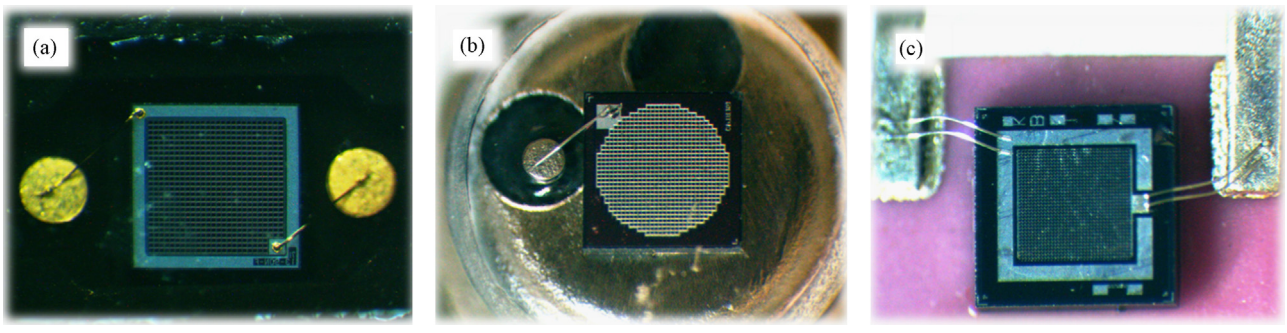

Fig. 3. Microscopic views of SiPM surfaces from different manufacturers: (a) Hamamatsu (MPPC S10362-13-050, $1.3 \times 1.3\ \mathrm{mm}^2$) [13], (b) CPTA (CPTA 143, $d = 1.3$ mm) [14], (c) MEPhI/PULSAR ($1.0 \times 1.0\ \mathrm{mm}^2$) [15].

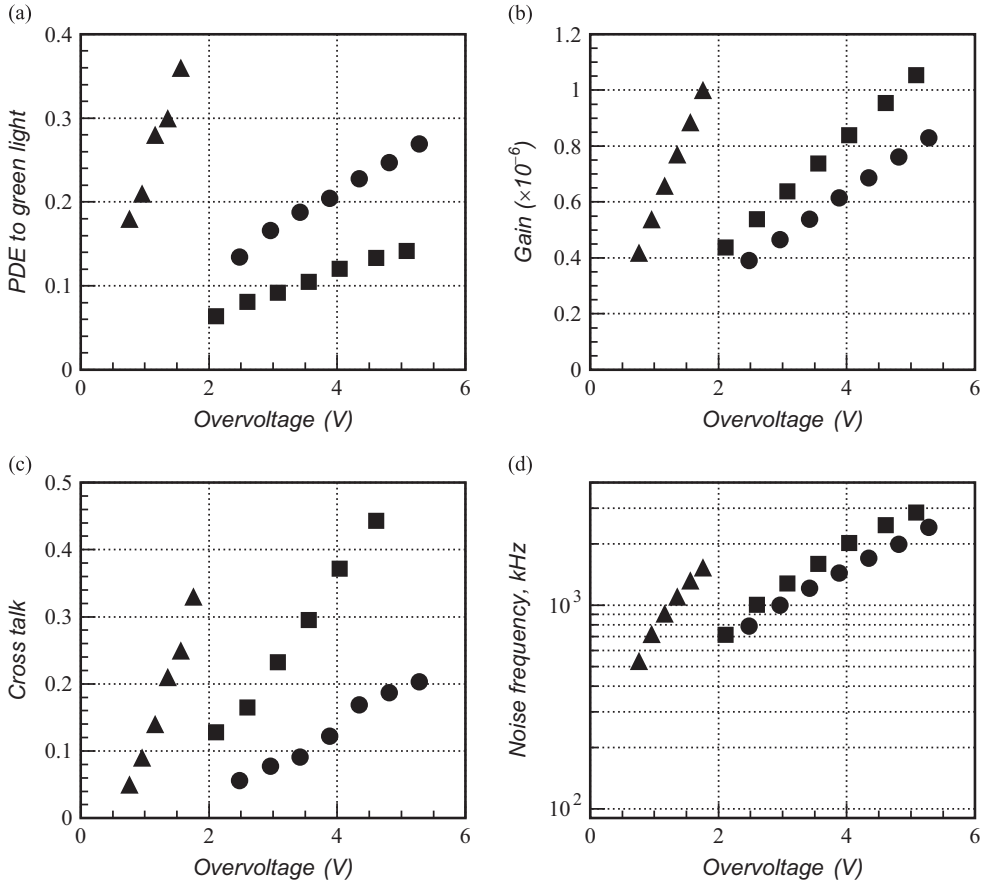

Fig. 4. Overvoltage dependence of SiPM (a) efficiency, (b) gain, (c) cross talk and (d) noise frequency for photo-detectors from different manufacturers: Hamamatsu (triangles), CPTA (circles), MEPhI/PULSAR (squares).

with geometry and scintillator plastic similar to ours [7,8,12]. The light emission spectrum of the Kuraray Y11 fiber is, in fact, quite well-matched to the SiPM spectral efficiency.

The strips have been tested using a cosmic ray stand. The cosmic ray trigger is provided by a pair of short trigger strips ($L=16$ cm) placed above and below the strip being measured. The trigger strips were moved along the tested strip to measure the light yield as a function of the distance to the photodetector. All strips were tested using SiPMs from the same vendor in order to minimize systematic errors. To determine the average number of detected photons, we correct the measured number of fired pixels by the cross-talk fraction $(1/(1+\delta)\sim 0.85)$ and conservatively use a truncated mean of the Landau distribution, discarding 10% of the lower portion of the distribution and 30% of the higher portion, then take the average of the resulting samples. The resulting averaged number, which is very close to the maximum of the spectra, is then corrected by a factor of 0.87 for oblique incidence of cosmic-ray muons, determined using a toy Monte Carlo simulation.

The distribution of the average number of detected photons is shown in Fig. 5a as a function of the distance to the photodetector (Hamamtsu MPPC S10362-13-050). We compare our results with the performance of the Fine-Grained Detectors (FGD) of the T2K experiment [23], where strips of the same length and the same SiPMs were used similarly. The scintillator light at the FGD is collected from the Fermilab strips (10×10 mm^2) using diameter 1 mm fibers. The light yield achieved is presented in the FGD TDR (Fig. 6 of Ref. [23]). Those tests were done in 120 MeV/c beams and then corrected, in the case of both muons and pions, for the expected MIP response. The light yield dependence on the distance to the photodetector in our case nicely agrees with the FGD test results. The light yield at the near end of the strip is $\sim$21 photoelectrons/MIP for FGD detector. We achieve a slightly higher light yield in spite of the four times larger strip width in our case (the light yield decreases with increasing width). We attribute this significant improvement in the light collection efficiency to the larger diameter of the fiber (light yield $\propto$ diameter) and the gluing of the fiber to the strip.

The Fermilab and Uniplast strips, which have the same price per unit weight, provide almost the same light yield at the SiPM, despite the fact that the Uniplast strips are 30% thinner. Apart from considerations of cost and weight of the entire system, the smaller scintillator thickness is beneficial in terms of reducing the neutron background. Indeed, the neutron rate is proportional to the scintillator volume. This consideration motivated our final selection of the Uniplast strips for the Belle II EKLM construction.

The transverse uniformity of the Uniplast strip response was measured using tightly collimated and triggered ^{90}Sr radioactive sources. Fig. 5b shows the relative pedestal-subtracted ADC response, which is proportional to the light yield, for two strips mechanically pressed against each other. The nonuniformity of the response is $\pm 25\%$. A reduction in the number of registered photons is observed near the groove, where the effective thickness of the scintillator is smaller, and at the strip edge, where the efficiency for scintillator light to reach the WLS fiber is smaller. From these results, we conclude that the light yield is adequate, irrespective of where a particle hits the strip.

In the same test we also measured the optical cross-talk between two neighboring strips. We used the ADC spectrum of the non-irradiated strip, when the collimated beam was placed at least 5 mm away from the common edge (otherwise the angular divergence of the beam may result in real scintillation in the strip under consideration). From the measured yield, we conclude that the optical cross-talk is $(3\pm 1)\%$.

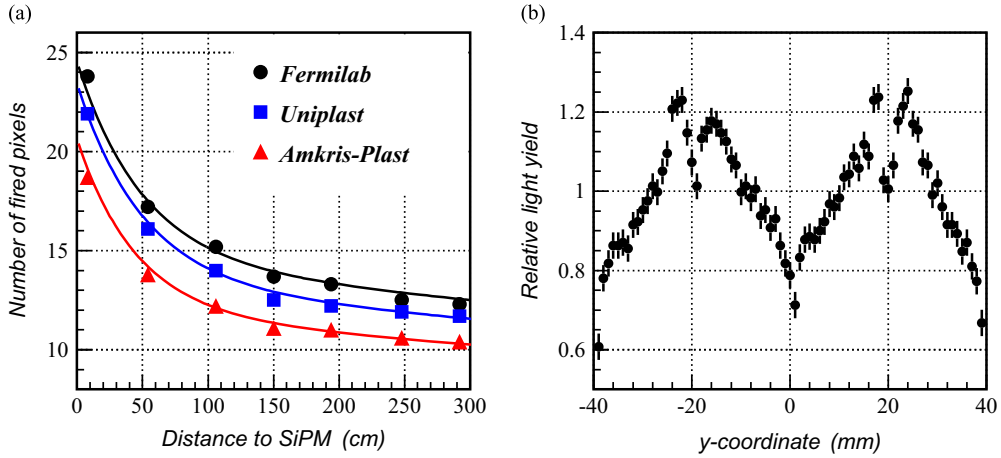

Fig. 5. (a) Distribution of the average number of SiPM-detected photons as a function of the distance to the photodetector. (b) The dependence of the relative light yield on the transverse position of the hit for two neighboring strips.

We measure the time resolution using a cosmic-ray trigger for a strip read out by two SiPMs, one on each fiber end. A TDC was started by one SiPM signal and then stopped by the second. From the observed time difference distribution, we can derive a time resolution $\sigma_t \approx 0.7$ ns. The measured velocity of light propagation in the WLS Y11 Kuraray fiber with 1.2 mm diameter is $v = 17$ cm/ns, which translates into $\sim$12 cm of spatial resolution along the strip.

3. Long-term stability and radiation hardness

Scintillator counters with WLS fiber using standard PMT read-out are used in many existing detectors, including those at hadron colliders, where the radiation dose is a few orders of magnitude higher than that anticipated at SuperKEKB. Such counters typically operate without degradation for decades. For example, the light collection of electromagnetic calorimeters for the HERA-B and LHCb experiments is based on Uniplast scintillator tiles read out by Kuraray Y11 fibers [24]. During several years of operation, no deterioration of the electromagnetic calorimeter performance was observed [25].

SiPMs demonstrate excellent long-term stability. Our experience in operating the 7620-channel CALICE hadron calorimeter prototype using scintillator/WLS fiber/SiPM detecting tiles during 3-year beam tests at CERN and FNAL [10,11] showed no significant deterioration of performance. Only 8 dead channels (0.1%) were observed, while the characteristics of the remaining channels were acceptably stable. The long-term stability of Hamamatsu SiPMs was tested in the T2K experiment, where $\sim$65 thousand channels were studied during a few years of operation. Failure was observed in $\sim$20 channels, *i.e.* less than 0.03%, primarily owing to mechanical damage.

However, the adequacy of SiPMs radiation hardness for our application needs to be proven experimentally. In particular, the radiation hardness of SiPMs was measured to be high in the case of irradiation with electrons and photons, while neutrons and protons cause significant damage at a moderate integrated dose of $\sim$1 kRad [10,26]. Typical radiation damage consists of defect formation in the thin area from which charge carriers are collected, resulting in an increase of the SiPM noise rate and, consequently, the dark current. Overall, the SiPM dark current grows linearly with particle flux as in other silicon detectors.

3.1. Study of scintillator strips aging

The long-term stability of the light collection efficiency of strips with glued WLS fibers was determined using a test module consisting of 96 strips (1 m long), manufactured in 2006. This test module was used for the measurement of the neutron background in the KEKB tunnel for a period of 6 months. Modules were placed in a 'hot' region and accumulated a dose corresponding roughly to 3–5 years of Belle II operation. In 2009, these strips were retrieved and examined for radiation damage and aging. No measurable degradation of the light yields (using new, not irradiated SiPMs) within the 10% accuracy of the measurements was observed 3 years after production. We also subjected a short strip with glued WLS fibers to fast aging in a thermostat at a temperature 80 °C during 4 months (corresponding to 10 years at room temperature according to Van tHoff's rule) and again found no noticeable aging effects.

3.2. SiPM's aging

Given the relative novelty of SiPMs, we have studied their radiation hardness in detail, including any possible deterioration as a function of particle type to which they are subjected. Radiation damage from protons and neutrons is energy-dependent and difficult to predict without knowledge of the beam background spectra. Therefore, to measure possible damage to SiPMs due to the high radiation levels anticipated at SuperKEKB, we performed radiation tests directly in the KEKB tunnel. Eight SiPMs produced by Hamamatsu and eight CPTA SiPMs were placed, for 6 weeks, in the KEKB tunnel at a location where the dose is much higher than in the nominal SiPM position. The integrated neutron dose at the tunnel measured with Luxel badges (J-type) [27] was $\sim$1.2 Sv. After irradiation, the SiPM dark current increased for both Hamamatsu and CPTA devices by a factor of 3.6 with small dispersion ($\sim$15%), as measured in 8 specimens.

The neutron dose was also measured near the nominal *in situ* position of the SiPM. The measured dose varies from 0.8 to 2.0 mSv/week at a luminosity $\mathcal{L} \sim 2 \times 10^{34}$ cm^{-2} s^{-1}. Assuming conservatively that the neutron dose increases linearly with luminosity, the expected neutron dose integrated over 10 years of SuperKEKB operation at $\mathcal{L} \sim 8 \times 10^{35}$ cm^{-2} s^{-1} does not exceed 40 Sv.[2] The extrapolated factor of dark current increase after 10 years of SuperKEKB is therefore $\sim$120. In the case of the Hamamatsu SiPMs, the expected dark current is $\sim$12 μA. In the case of the CPTA SiPMs, the dark current becomes much higher ($\sim$170 μA), since the initial noise is higher for the CPTA SiPMs. The difference between the Hamamatsu and CPTA SiPMs can be explained by the different thicknesses of the sensitive zone and

[2] Monte Carlo simulation of the radiation dose actually predicts a dose which varies more slowly than linearly.

the difference in manufacturing details (purity of the raw materials and also of the SiPM surface) on which both the initial noise and the performance depend.

The study of SiPM properties after irradiation was done at the Institute for Theoretical and Experimental Physics (ITEP) in Moscow. The SiPMs were subjected to fast irradiation in the 200 MeV secondary proton beam of the ITEP synchrotron ($\sim 10^{10} p/\mathrm{cm}^2/\mathrm{hour}$). One month after irradiation, the Hamamatsu SiPM dark current was measured to be 16 μA (corresponding to more than 10 years of operation at SuperKEKB) for two specimens subjected to an integrated proton flux $2.0 \times 10^{11} p/\mathrm{cm}^2$ and 6.5 μA (corresponding to 5 years of operation at SuperKEKB) for two specimens subjected to an integrated proton flux $7.4 \times 10^{10} p/\mathrm{cm}^2$.

We studied the light yield from minimum-ionizing particles traversing the far end of the strip (~3 m from the photodetector) detected with both non-irradiated and also irradiated SiPMs. The average number of photoelectrons (p.e.) obtained from a MIP signal using irradiated and control SiPMs is unchanged, though in the case of irradiated SiPMs, the MIP signal is slightly smeared owing to increased noise. The dependence on the threshold of the efficiency at the far end of the strip, as well as the noise rate, in terms of the number of photoelectrons, is presented in Fig. 6. We conclude that the light detection efficiency is not significantly changed after irradiation, while the internal noise rate increases significantly. However, at a threshold of ~7.5 fired pixels the background rates from increased SiPM noise remain smaller (≲10 kHz) than the physical background rate due to neutron hits in the scintillator (≲160 kHz for the longest strip). The MIP detection efficiency is similar with irradiated CPTA's SiPM, but the noise rate becomes unacceptably high (100–500 kHz).

We therefore conclude that the Hamamatsu's SiPM radiation hardness is sufficient for successful EKLM operation at the design SuperKEKB luminosity for at least 10 years. The significantly increased dark current, however, should be considered in the design of electronics, HV supplies, slow control and the calibration procedure. This work is currently underway.

4. Improving light collection efficiency

In the previous sections, we have demonstrated that commercially available SiPMs provide the basis for an adequate KLM detector system at the Super KEKB factory. However, given the expected dispersion of strip characteristics during mass production, and to also ensure better robustness and physics performance, we further studied the possibility of improving the light collection efficiency at the SiPM. We carefully studied two points in the system where there may be loss of light: in the transport of scintillator light to the WLS fiber, and the subsequent conveyance of the WLS fiber light to the SiPM.

The effective transport of the scintillator light to the WLS fiber is improved with the help of the optical glue, which has refractive index similar to that of both the strip and the outer cover of the fiber. The glue significantly reduces the light loss due to the roughness of the mating surface. However, it is very difficult to fill the corners of the rectangular groove even with very low-viscosity glue, resulting in small residual air bubbles at the groove corners, and therefore enhanced scattering and absorption of photons in this region. This problem does not arise if the shape of the groove is rounded. By milling the groove to a rounded shape, our lab tests demonstrate an increase in the average detected light yield by $(25 \pm 5)\%$ relative to the "standard" rectangular-shaped grooves.

The optical contact between the WLS fiber end and the SiPM can be also improved. The SiPM matrix is covered with a thin protective resin. The optimal configuration of the optical contact corresponds to the minimal air gap between the fiber end and this cover, while avoiding mechanical contact so as not to damage the cover. We studied the flatness and thickness variation of this cover using a microscope, and found that the shape of the cover in the case of the Hamamatsu SiPMs is not flat, but concave (see Fig. 7a), which is consistent with surface tension effects during the hardening of the resin. As a result, the light from the fiber is defocused at the SiPM matrix – this effect is actually aggravated in practice, as the air gap turns out to be much larger than that expected for the flat cover. We measured the dependence of the light yield at the SiPM on the length of the fiber inside the SiPM (Fig. 7b). This effect turns out to be substantial: a 150 micron extension to compensate for the concavity of the resin (which still ensures no mechanical contact of the fiber end to the resin surface) results in a $(37 \pm 5)\%$ increase of the number of photoelectrons detected at the SiPM.

As a result of these studies, we improved the light collection efficiency by ~70%, by implementing the straightforward modifications to the strip production technology described above.

5. Physics performance

Besides the main mission to detect K_L^0 mesons and muons, another important task for the KLM system at Belle II, motivated by our extensive Belle experience, is to serve as an hadronic veto

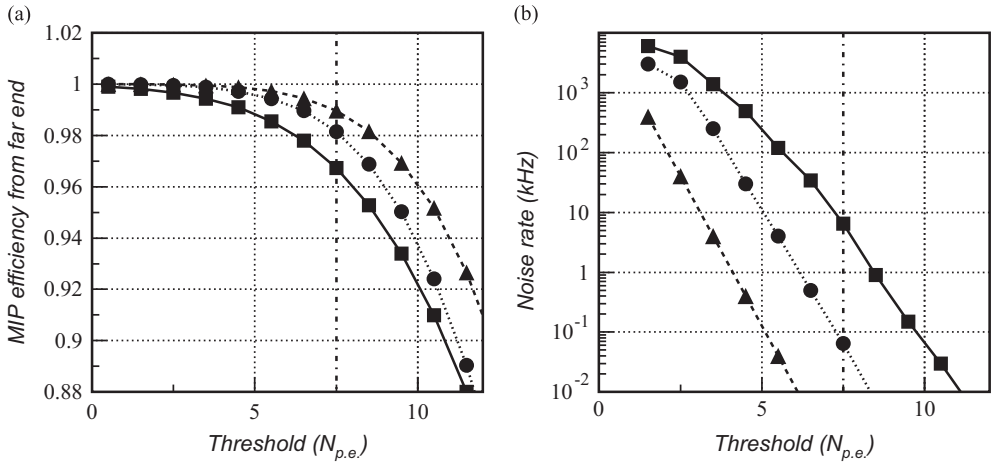

Fig. 6. Dependence on the threshold (defined by the number of photoelectrons) of (a) the MIP detection efficiency from the strip far end and (b) the internal noise rate for Hamamatsu SiPMs. The triangles correspond to the non-irradiated SiPMs; circles correspond to SiPMs irradiated with a $7.4 \times 10^{10} p/\mathrm{cm}^2$ dose (corresponding to 5 years of operation at SuperKEKB) and the squares show the case for an SiPM irradiated with $2.0 \times 10^{11} p/\mathrm{cm}^2$ dose (more than 10 years of operation at SuperKEKB).

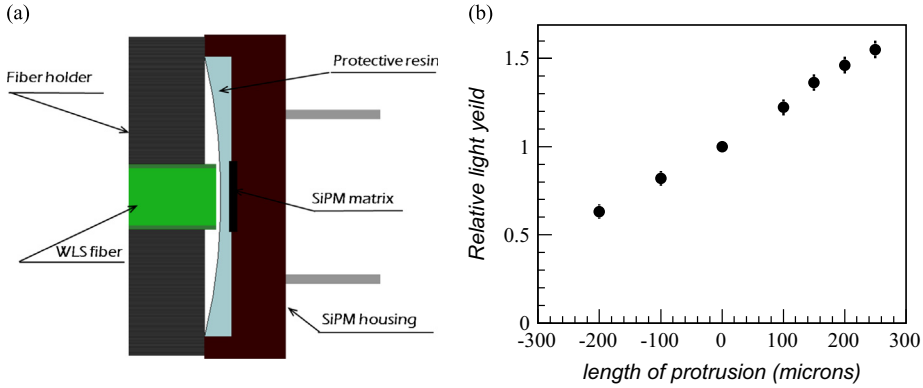

Fig. 7. (a) Schematic view of the optical connection of the WLS fiber end and SiPM (Hamamatsu MPPC S10362-13-050); (b) relative light yield dependence on the length of the protrusion (normalized to zero protrusion).

to improve the signal to background ratio for the so-called missing energy modes, such as $B^+ \to \tau^+ \nu$, $B \to K^{(*)} \nu \bar{\nu}$, *etc.* [28]. Indeed, the major background remaining after baseline selection for these modes is due to B-decays with missing neutrals or unreconstructed charged hadrons. In this case, a veto on KLM hadronic clusters would be very useful, provided a high efficiency and low background can be achieved with the new KLM system.

The muon identification and hadron cluster reconstruction performance depends on the background rate, mostly related to slow neutrons produced in the accelerator tunnel and in the vicinity of the interaction region. In spite of the much higher sensitivity to neutrons for scintillators containing hydrogen compared to the gas+glass based RPC, the total background rate of the new EKLM system is expected to be much lower than those achievable with RPC design. Indeed, single background neutrons are usually absorbed in one scintillator strip, so there are no two-dimensional hits from single background particles; fake two-dimensional hits mostly arise from random coincidences within the integration time. This is in contrast to RPCs, where even a single scattered neutron induces signals on both stereo strips.

To estimate the background rate we have used two independent methods: (i) a conservative extrapolation of the measured neutron rates using a scintillator test module and (ii) a Monte Carlo detector study.

5.1. Measurement of the background neutron rate

As RPC and scintillators have different responses to beam backgrounds, an extrapolation of the known Belle background rate at the RPC to the expected rate at the scintillator KLM at SuperKEKB is difficult. We have therefore performed measurements of the neutron flux using a scintillator test module installed directly in the KEKB tunnel close to the EKLM. The test module contained four layers. Each layer, surrounded by a copper shielding box (4 cm thickness) for protection from external light and soft electron/photon backgrounds, was assembled from 24 strips. Each scintillator strip, with a WLS fiber and SiPM readout, had a size of $1000 \times 40 \times 10$ mm^3. During KEKB operation, the signals from 96 channels were collected by random triggers using CAMAC ADCs, with a gate set to be 100 ns.

We found that a simple shielding box was inadequate for protecting the module from numerous charged tracks and showers. To discriminate neutron signals from other sources, different hit patterns in the four layers were used. A significant portion of the observed events (where at least one SiPM signal exceeds the threshold of 0.5 MIP) had multiple hits from charged tracks or showers; to suppress such backgrounds, we required a veto in the two outer layers and also required a single hit in one of the two inner layers. The derived neutron rate at a nominal 0.5 MIP threshold, at a luminosity of $\mathcal{L} \sim 1.4 \times 10^{34}$ cm^{-2} s^{-1}, was 6 Hz/cm^2. We use this number to estimate the expected occupancies in the readout electronics and trigger (maximum 160 kHz from the longest strip, 60 kHz averaged), as well as to estimate the expected backgrounds for K_L^0 reconstruction.

5.2. Monte Carlo simulation

The new endcap KLM detector geometry has been coded into the GEANT4 package [29], which then simulates the energy deposition of signal hits in each strip. Both signal events and neutron background were simulated in this way. For the neutron background, a ± 6 m accelerator tunnel side was simulated, including a realistic description of the SuperKEKB optics and also including radiative Bhabhas, the Touschek effect, and other background sources. The response of the KLM system to the energy deposition is simulated based on our test measurements. We assume that multiple hits at the same strip are correctly resolved by the readout electronics if their arrival time difference is greater than 10 ns, otherwise they are merged into one hit. Hit information is stored for further analysis if the amplitude exceeds the threshold of 7.5 p.e.

The background induced by neutrons turned out to be slightly lower than those obtained from our conservative extrapolation described above, corresponding to a maximum 120 kHz rate for the longest strip. For our background studies, we assume that hits are distributed uniformly in time. We use similar procedures to digitize both background and signal hits.

5.3. Superlayer cluster reconstruction

The KLM hit reconstruction procedure is similar to that used in the Belle reconstruction software. We exploit the improved time resolution that can be achieved with the new electronics and DAQ [30].

Neighboring hit strips in the same plane with hit time difference smaller than 10 ns are grouped to form a 1D hit with coordinate defined as the weighted average over the hit-strips' coordinates. Two 1D hits from orthogonal layers in the same superlayer that intersect spatially and match in time form a '2D hit'. The reconstructed 2D hits from all superlayers are used for muon and K_L^0 reconstruction.

5.3.1. Muon identification

The muon identification procedure, for muons exceeding the detection threshold of 0.6 GeV/c, is based on the extrapolation of

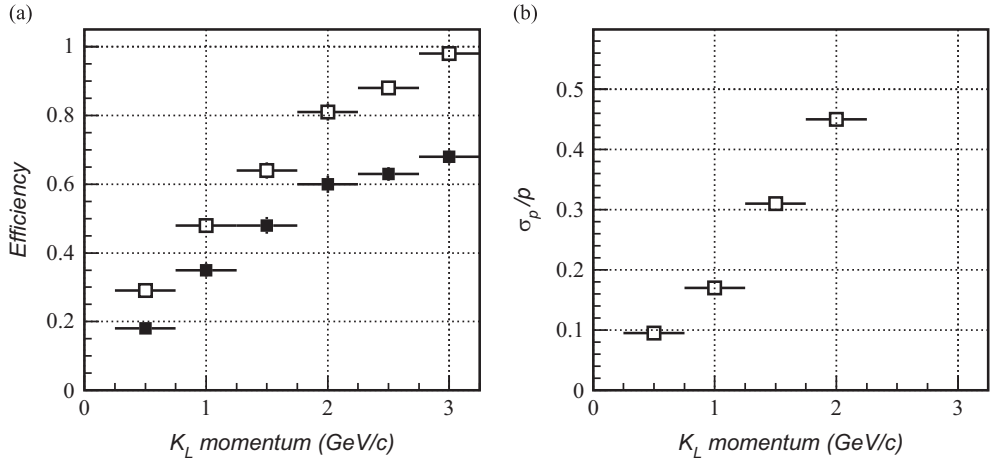

Fig. 8. K_L^0 reconstruction: (a) efficiency of K_L^0 cluster-finding with a tight requirement of two 2D-hits in different superlayers (hatched squares) vs. a loose requirement of ≥ 1 superlayers hit (open squares); (b) momentum resolution.

reconstructed charged tracks outward from the Belle II drift chamber into the KLM detector. The muon identification procedure then compares the likelihoods of muon vs. hadron hypotheses, based on the longitudinal and transverse profiles of the extrapolated tracks to EKLM 2D hits within some geometric matching requirement.

Misidentification is mainly due to hadronic showers and pion or kaon decay in flight, which is thus largely independent of the KLM detection technique. However, the expected efficiency of the scintillator EKLM detector is slightly higher than for the previous Belle EKLM; we therefore expect that the muon identification performance should be slightly improved.

The measured muon detection efficiency and pion fake rates are approximately constant for momenta greater than 1.0 and 1.5 GeV/c, respectively. Between 1.0 and 3.0 GeV/c the average muon detection efficiency is 90% and the hadron fake rate is less than 1.5% over the KLM acceptance, using the standard likelihood selection criterion $\mathcal{L} > 0.9$.

5.3.2. K_L^0 reconstruction

Following the procedure used at the Belle experiment, K_L^0 clusters are reconstructed as a group of 2D hits within a 5° cone angle relative to the interaction point, which are compatible in time with being produced by a single nuclear shower. As in the algorithm used at Belle we require 2D hits in at least two superlayers. The efficiency for K_L^0 cluster-finding in the KLM is shown in Fig. 8a as a function of K_L^0 momentum. The angular resolution is ~10 mrad over a wide momentum range, which is approximately the same as for the Belle system.

The main source of K_L^0 fake candidates is the random coincidence of 1D hits induced by neutrons. After SiPM irradiation, some small contribution to fake candidates arises from the increased SiPM noise. We find $\ll 0.01$ fake K_L^0 candidates per event at the design luminosity. Given that the fake rate is negligibly small, we have studied the possibility of increasing the K_L^0 efficiency by loosening the cluster selection, allowing 2D hits in only one superlayer. This results in increased K_L^0 efficiency by up to 30% (Fig. 8a, open squares), while maintaining the background rate at a relatively low level (< 0.2 fake cluster/event). Further fake cluster rate suppression can exploit both amplitude information, as well as the one-superlayer hit pattern characteristics, depending on the signal-to-noise requirements of a particular analysis.

We can also take an advantage of the good scintillator time resolution to determine the K_L^0 momentum using the EKLM system as a time-of-flight detector, at least for medium-momentum kaons. The resulting momentum resolution as a function of K_L^0 momentum is shown in Fig. 8b. The timing measurements provide useful information for kaons with momenta up to 1.5 GeV/c.

Based on the simulation we conclude that the new EKLM detector provides even better performance for K_L^0 reconstruction than the old one, and thus also an improved hadronic veto for the study of important B decay modes with neutrinos in the final state.

6. Conclusion

We have studied a system based on scintillator counters with WLS fiber light collection and SiPM readout for the Belle II experiment. We have identified a few simple improvements in the strip production technology which allow significant increases in the light collection efficiency, thus increasing the efficiency and robustness of the entire detector. The new system should work efficiently at background rates and radiation doses ~100 times larger than those observed for the Belle experiment. As demonstrated by many tests described herein, the system has sufficient robustness to operate well in a strong magnetic field and high radiation and interaction environment with no significant degradation anticipated after many years of data-taking. While this system was designed for a particular experiment, namely Belle II, our study can be applied to the construction of muon systems in many experiments. For example, our experience is being used in the design of the cosmic ray muon veto system for the COMET experiment [31]. It was also considered during the design of the muon system of the ILD experiment at the International Linear Collider (ILC) [32].

Acknowledgments

It is our pleasure to thank K. Abe and K. Sumisawa for their invaluable help with carrying out of tests of the module at KEK. The work is supported by the Russian Ministry of Education and Science contracts 14.A12.31.0006 and 4465.2014.2 and the Russian Foundation for Basic Research grant 14-02-01220.

References

[1] S. Hashimoto, et al. (Eds.), Letter of Intent for KEK Super B Factory (Part-II, Detector), KEK Report 04-4, 2004.
[2] T. Abe, et al., The Belle II Technical Design Report, KEK Report 2010-1, 2010, arXiv:arXiv:1011.0352.

[3] A. Abashian, et al., Belle Collaboration, Nuclear Instruments and Methods in Physics Research Section A 479 (2002) 117.
[4] A. Abashian, et al., Belle Collaboration, Nuclear Instruments and Methods in Physics Research Section A 449 (2000) 112.
[5] V. Balagura, et al., Nuclear Instruments and Methods in Physics Research Section A 564 (2006) 590.
[6] M. Andreotti, et al.,IEEE Nuclear Science Symposium Conference Record 1718, 2010.
[7] I. Ambats, et al., Minos Collaboration, FERMILAB-DESIGN-1998-02, 1998.
[8] R. Acquafredda, et al., Opera Collaboration, The Journal of Instrumentation 4 (2009) P04018. http://dx.doi.org/10.1088/1748-0221/4/04/P04018.
[9] A. Akindinov, et al., Nuclear Instruments and Methods in Physics Research Section A 387 (1997) 231;
G. Bondarenko, et al., Nuclear Physics B—Proceedings Supplements B 61 (1998) 347;
V. Saveliev, V. Golovin, Nuclear Instruments and Methods in Physics Research Section A 442 (2000) 223;
G. Bondarenko, et al., Nuclear Instruments and Methods in Physics Research Section A 442 (2000) 187;
Z. Sadygov, et al., Nuclear Instruments and Methods in Physics Research Section A 504 (2003) 301;
V. Golovin, V. Saveliev, Nuclear Instruments and Methods in Physics Research Section A 518 (2004) 560.
[10] M. Danilov, Nuclear Instruments and Methods in Physics Research Section A 581 (2007) 451.
[11] F. Sefkow, PoS PD07:003, 2006.
[12] Y. Kudenko, et al., T2K Collaboration, Nuclear Instruments and Methods in Physics Research Section A 598 (2009) 289.
[13] Hamamatsu Photonics K.K. (Japan), ⟨http://www.hamamatsu.com/eu/en/index.html⟩.
[14] CPTA, Ltd. (Russia), ⟨http://www.cpta-apd.ru/eng/index.html⟩.
[15] Research and production enterprise PULSAR, ⟨http://www.pulsarnpp.ru/index.php/fotoelektronika⟩ (in Russian).
[16] V. Andreev, et al., Nuclear Instruments and Methods in Physics Research Section A 540 (2005) 368.
[17] Saint-Gobain, Ltd. (France), ⟨http://www.crystals.saint-gobain.com/Plastic_Scintillation.aspx⟩.
[18] AMCRYS-H Co. (Ukraine), ⟨http://www.amcrys-h.com/index.htm⟩.
[19] A. Pla-Dalmau, et al., MINOS Scintillator Group Collaboration, Frascati Physics Series 21 (2001) 513.
[20] Research and production enterprise UNIPLAST (Russia), ⟨http://uniplast-vladimir.com/index.php?page=scint⟩ (in Russian).
[21] Kuraray, Ltd. (Japan), ⟨http://kuraraypsf.jp/psf/ws.html⟩.
[22] Research and production enterprise SUREL, Ltd. (Russia), ⟨http://www.surel.ru/silicone/36-surel-sl-1.php⟩ (in Russian).
[23] P.-A. Amaudruza, et al., T2K Collaboration, Nuclear Instruments and Methods in Physics Research Section A 696 (2012) 1.
[24] A. Zoccoli, et al., Hera-B Collaboration, Nuclear Instruments and Methods in Physics Research Section A 446 (2000) 246;
A.A. Alves Jr., et al., LHCb Collaboration, The Journal of Instrumentation 3 (2008) S08005.
[25] see eg. P. Perret, arXiv:arXiv:1407.4289.
[26] E. Tarkovsky, PoS PD07 013, 2006.
[27] Landauer, Ltd. (Japan), ⟨http://www.landauer.com/Industry/Products/Dosimeters/Dosimeters.aspx⟩.
[28] T. Aushev, et al., arXiv:arXiv:1002.5012.
[29] S. Agostinelli, et al., GEANT4 Collaboration, Nuclear Instruments and Methods in Physics Research Section A 506 (2003) 250;
J. Allison, et al., GEANT4 Collaboration, IEEE Transactions on Nuclear Science NS-53 (2006) 270;
⟨http://www.geant4.org/geant4⟩.
[30] See talk by G. Varner: ⟨http://www.phys.hawaii.edu/∼idlab/taskAndSchedule/KLM/KLM_electronics_CDR.pdf⟩.
[31] O. Markin, E. Tarkovsky, arXiv:arXiv:1402.5522.
[32] T. Behnke, et al., arXiv:arXiv:1306.6329.